Journal of Renewable Energy and Sustainable Development (RESD) Volume 10, Issue 2, December 2024 - ISSN 2356-8569
http://dx.doi.org/10.21622/RESD.2024.10.2.1019

Received on, 17 September 2024 Accepted on, 31 October 2024 Published on, 27 November 2024

Utilizing Maritime Caves for Wave Energy: Wells Turbine Performance and Household Power Supply from Cave-Generated Electricity

Wilson M. L. Monteiro [1,*], António Sarmento [2], Bruno Semedo [3], Arider Carvalho [4], Tomás Tavares [5], and Jakson A. L. Monteiro [6]

[1,3,4,5,6] Faculty of Science and Technology, University of Cape Verde, Praia, Cape Verde

[2] WavEC - Offshore Renewables, Edifício Diogo Cão Doca de Alcântara Norte 1350-352, Lisbon, Portugal

wilson.monteiro@docente.unicv.edu.cv, antonio.sarmento@wavec.org, bruno.semedo@unicv.cv, arider.carvalho@student.unicv.edu.cv, tomas.tavares@docente.unicv.edu.cv, jakson.monteiro@docente.unicv.edu.cv

ABSTRACT

Maritime Natural Caves (MNCs) are coastal infrastructures that harness ocean wave energy to generate pneumatic power, which drives a turbo-generator to produce electricity. This study focuses on the use of MNCs for wave energy extraction, with the Cidade Velha MNC identified as the most promising one. The research involved constructing several Wells turbines with varying rotor blade orientations (β) to analyse their impact on energy production during high-energy conditions within the MNC. The characteristic curves of the turbines show a linear trend, with determination coefficients exceeding 75%. However, non-linear behaviour was observed at higher flow rates probably due to boundary layer separation on the turbine blades. Quadratic data approximations provided a better fit, with determination coefficients over 93%. Among the turbines tested, the one with a 15° blade inclination (β=15°) was more effective under extreme conditions, followed by the β=0° turbine, while the turbine with a 5° inclination (β=5°) was less suitable. Despite its better performance in high-energy conditions, the turbine with β=15° encountered more start-up difficulties and longer downtime compared to the β=0° turbine, which performed better under low to moderate energy levels. The turbines with blades inclined at β=15° and β=0° achieved maximum efficiencies of 369 and 273.8, respectively. However, as evidenced by the researchers' data, these high efficiencies were influenced by the inertial effect of the turbines and the hysteresis to which the natural cave was subjected. Additionally, the turbines experienced operational issues at high rotational speeds. The initial attempt to use MNCs for household electricity generation revealed several challenges that must be addressed before MNCs can be considered reliable energy sources.

Index-words: *Maritime Natural Cave, MNC production, Wells turbines, Hysteresis, Cidade Velha MNC power plant.*

I. INTRODUCTION

It is estimated that the global potential for wave energy is around 30,000 TWh/year, surpassing the world's electricity consumption. Since waves are an abundant natural resource, many devices have been developed to convert this energy into electricity. These devices can be classified into three main categories: Point Absorbers, which account for about 46% of the total; Oscillating Wave Surge, which represent around 16%; and Oscillating Water Column devices, which make up 15% of the existing technologies (Koca, et al., 2013).

Most of these devices use electromagnetic generators to produce electricity. However, these generators require high and stable frequencies (50-60 Hz) to operate efficiently (Wang, 2917; Yao, 2016). As a result, they do not perform well under waves with low frequency, low amplitudes, irregularities, or random directions. Due to these limitations, recent advancements have introduced new technologies for generating electricity from ocean waves. Among these, triboelectricity, piezoelectricity, and electromagnetism stand out (Barua and Rasel, 2024).

The triboelectricity has gained special attention with the invention of triboelectric nanogenerators (TENGs) by Professor Wang Zhonglin (Wang et al., 2017). These devices offer several advantages in low-frequency wave environments, being lightweight, low-cost, simple in structure, and pollution-free. However, due to their small size, large-scale

Volume 10, Issue 2, December 2024 - ISSN 2356-8569
http://dx.doi.org/10.21622/RESD.2024.10.2.1019

application in open oceans requires integrating these generators into networks, a challenge still under investigation. Another key aspect is the efficiency of these generators, which needs to be improved to enable widespread use.

The large-scale implementation of TENGs systems also demands a significant amount of connecting cables, which can increase the system's costs. Furthermore, the wear of triboelectric materials in the marine environment is another challenge that must be addressed to enhance the durability and long-term viability of these generators (Wang, 2917; Yao, 2016).

The main challenge in the wave energy market is financial. It has been expensive to develop the technology. The CorPower device, for example, spent about 30 million Euros to reach Technology Readiness Level 8 (TLR8) (CorPower, 2023). Cost-wise, there is also a risk they might not be able to compete with other renewable energy technologies, and it takes a long time to get everything set up for the market (Cruz and Sarmento, 2004). This situation becomes even more critical as fixed-platform offshore wind energy approaches electricity competitive production, with energy selling prices close to 50 Euros/kWh. Moreover, floating wind energy is increasingly emerging as a mature technology with significant potential for competitiveness within a period of 5 to 10 years (Bošnjakovic *et al*., 2022). The existence of an alternative that provides the same as wave energy, with lower risk, lower development costs, and a shorter time to market, diverts investment sources from wave energy that could otherwise contribute to its development.

The reason for the high investment cost of wave energy plants is the requirement of expensive technologies to convert the energy, as well as costly structural and mechanical components. In this situation, around 80% of the initial cost is used for the construction and mechanical parts of the plant. Thus, there is a real need to find ways to reduce this starting cost, which would make this renewable energy type more attractive. According to Table I, which presents the expected changes in costs for setting up wave energy systems and generating electricity from ocean waves as seen in 2003, the researchers would have thought that the costs related to wave energy would go down significantly by 2020 (Wavenet, 2003). However, that did not happen. The cost of generating electricity from ocean waves remains high compared to other sources of renewable energy. One of the reasons for this behaviour is the lack of sufficient investment in this technology. This happened because of the global financial crisis in the late 2000s, which affected money availability in the early 2010s. Also, the innovative nature of many of its systems and subsystems, failures on some of the technologies tested and the relatively small size of the devices contributed to a reduction in the investment in wave energy. Also, the growth of offshore wind energy in the later part of the same decade played an important role by promoting electricity production at a lower cost and thus deviating investment from wave energy.

TABLE I
EVOLUTION OF INSTALLATION AND ELECTRICITY COSTS OF WAVE ENERGY POWERPLANTS.

Year	Installation [Euro/kW]	Electricity [Euro/kWh]
2000	10000-20000	0.2-0.3
2006	5000-15000	0.1-0.2
2010	2000-10000	0.08-0.12
2020	1000-2000	0.03-0.05

For OWC facilities, one idea to install them at a lower cost is to build them into breakwaters whenever possible. This different procedure saves money during the setup and facilitates access to the facility for building and maintenance purposes. This technology was first implemented in 1990 in Japan (Sakata), and then it was replicated in Spain (at the Mutriku Port) between 2008 and 2010. Portugal also had plans to build a similar system at the Douro River breakwater, but those plans were not realized (Falcão, 2010).

The MNCs are spaces that form naturally under the rocks of the sea slopes, inside of which there are volumes of air constantly excited by the movement of the sea waves. Thus, the rise and fall of the free surface of the sea inside the MNCs promotes the compression and expansion of the air inside, inducing pressure values different from the local atmospheric pressure. Therefore, the air is forced to leave and enter these MNCs, whenever there is a hole in the rocky shoreline surface. The jets of air through the holes enable one to identify these natural infrastructures. The following figure shows a photograph of an MNC located in the Farol region, in Praia City (Santiago Island: Cabo Verde).

Volume 10, Issue 2, December 2024 - ISSN 2356-8569
http://dx.doi.org/10.21622/RESD.2024.10.2.1019

Fig. 1. MNC - Farol

Fig. 1 shows the exact manifestation of sea waves in an MNC, having a hole on its surface. The white cloud in the photograph shows the jet through the MNC orifice, which can be used to drive a turbo-generator set to produce clean electricity. In this case, the jet is a mixture of air and water droplets, which will be troublesome for the turbine as the water droplets will provoke abrasion in the turbine blades.

The purpose of using MNCs is to reduce the structural and construction costs of an OWC plant. In this case, there will be no need to change these natural structures, mostly made of rocks, to set up the plant. Since the pneumatic chamber is already there, the turbo-generator is just fitted into the cave orifice. Thus, it is only necessary to build a housing for the plant electrical equipment.

Brian Holmes, from University College Cork- UCC first presented the use of MNCs for wave energy extraction (Holmes, 1984). However, the work carried out by this researcher was interrupted due to a lack of funding and did not produce any practical results. It is important to underline that the idea of using the MNCs to produce electricity from the sea waves in Cabo Verde is innovative and independent of the work carried out by Brian Holmes. This idea is based on the possibility of reducing construction costs and improving the survival of classic OWC-type plants, using natural infrastructure (rocks) whose resistance has been tested over time by the aggressiveness of the sea waves.

The MNCs represent a natural form of Oscillating Water Column (OWC) devices that are fixed along the maritime slopes. Over the years, these devices have been the subject of numerous studies aimed at improving their performance by addressing the geometry of their pneumatic chamber (Lee and Chen, 2020; Yacob et al., 2022), the geometry of the air turbine that equips them (Falcão and Henriques, 2016), and the control of the airflow passing through the turbine (Rosati et al., 2022). Other studies have focused on reducing the investment cost of the plants formed by these devices by incorporating them into breakwaters, as done in Spain (Mutriku port) (Torre-Enciso et al., 2009) and Japan (Sakata power plant). There are also plans to implement this approach in Portugal (Falcão, 2010).

Few studies have specifically targeted the use of natural caves for harnessing wave energy. The first attempt in this regard did not yield visible results (Holmes, 1998). Monteiro et al. (2021, 2022) conducted the most significant studies in this context.

According to Monteiro et al. (2021), the operation of the natural cave at Cidade Velha is strongly influenced by tidal states. When tidal states evolve from high tide to low tide, all physical parameters associated with the manifestation of the cave decrease over time, including the pressure energy converted from wave motion. Conversely, the transition from low tide to high tide is accompanied by a successive increase in the pressure energy of the cave. The highest values of the average airflow velocity through the cave orifice (without the installation of the turbine) varied between 72.17 m/s and 84.20 m/s, and the maximum Mach number was around 0.33, which allows the flow to be considered incompressible. On average, the pneumatic power converted by the cave varied between 0.9 kW and 1.5 kW. However, the peak values of this parameter reached nearly eight times greater than the averages, ranging from 6.9 kW to 10.8 kW. The morphology of the coastline near the studied cave is convergent, causing an increase in the amplitude of the incoming waves. However, there are two partially submerged rocks in front of the cave that disturb the incoming waves, forcing them to break

Volume 10, Issue 2, December 2024 - ISSN 2356-8569
http://dx.doi.org/10.21622/RESD.2024.10.2.1019

and thereby dissipating the excitation energy of the cave.

Monteiro et al. (2021), using the average values of airflow velocity, designed a Wells turbine to operate with an electric generator of 1.1 kW, rotating at 2760 RPM and 50 Hz. Based on these data, a Wells Turbine with a rotor of horizontal blades (90 degrees relative to the turbine axis) was designed, with its specifications listed in Table II.

TABLE II
. GEOMETRICAL CHARACTERISTICS OF THE WELLS TURBINE (MONTEIRO ET AL., 2021).

Parameters	Values
σ	0.72
R_{tip} [mm]	207
R_{hub} [mm]	100
h	0.484
R_{mid} [mm]	100
N	4
c[mm]	173

In Table II σ, R_{tip}, R_{hub}, R_{mid}, h, c and N are, respectively, the solidity, tip radius, hub radius, mid radius, hub-to-tip radius ratio and the blade number of the turbine designed.

The designed Wells turbine was constructed entirely with materials available in the Cape Verdean market (Monteiro et al., 2022). After being adapted to the cave orifice, the characteristic curve of the turbine was obtained. It was found that the highest values of power at the turbine shaft ranged between 842 W and 1030 W and were obtained for flow coefficients varying from 0.2 to 0.34. The maximum efficiency of the system (pipes, turbine, and generator), η=30.8%, was achieved for a flow coefficient that is outside this range (φ=1.12). The maximum power at the turbine shaft was 1.03 kW and is associated with a flow coefficient of 0.46 and a conversion efficiency of η=29.3% (Monteiro et al., 2022). For maximum conversion efficiency, the power at the turbine shaft is relatively low, equal to 60 W. This discrepancy between the flow values for maximum power and maximum efficiency cannot be easily interpreted, as it would be expected that maximum power would occur for flow coefficients close to those of maximum efficiency, considering only the turbine's efficiency curve. However, some inaccuracies associated with our study may have caused this small discrepancy (Monteiro et al., 2022).

When a system reacts based on its previous state, it exhibits hysteretic behaviour (Skii, and Pokrovskii, 1989). Although the researchers' have not specifically studied the sources of hysteresis in the Cidade Velha MNC, the data from its energy profile allowed them to draw some important conclusions about this phenomenon in such infrastructures.

Studies on Oscillating Water Column (OWC) devices, which imitate the MNCs, have identified the air compressibility in the pneumatic chamber as the main cause of hysteresis. Other factors, such as the aerodynamics and the turbine inertia, exist but are less relevant. According to these studies, air compressibility causes a delay between the movement of the water piston inside of the pneumatic chamber and the airflow through the turbine, while the influence of turbine aerodynamics is minimal and independent of the turbine solidity. The same study suggests that hysteresis due to air compressibility is more significant, dependent on the turbine's solidity, and consequently even more significant in real OWC plants (Ghisu et al., 2016, 2017, 2020). Other studies indicate that hysteresis can be eliminated if the turbine performance is measured close to the rotor (Puddu et al., 2014).

Conversely, some research highlights turbine aerodynamics as a significant cause of hysteresis. Setoguchi et al. (1998) observed that the operation of the Wells turbine in reciprocating flow presents significant hysteresis, especially with greater turbine solidity, but it is insensitive to the Reynolds number and blade roughness. Kinoue et al. (2003) associated hysteresis with vortex formation near the blades, in the suction region.

The aim of this work is to explore the potential of natural caves as more economical alternatives for generating energy from ocean waves, compared to Oscillating Water Column (OWC) plants fixed on coastal cliffs. To achieve this, it will be necessary to complete a series of key steps, such as surveying some caves in Cabo Verde and selecting, based on specific criteria, those with the greatest potential for in-depth studies. These studies aim to assess the energy performance of the caves when equipped with Wells turbines of various geometries, especially during periods of intense wave activity, when wave energy is highest.

Another objective of this work is to analyze the operation of the cave with the Wells turbine installed and to draw conclusions that may guide improvements for future research at the site.

Finally, the researchers intend to use the studied cave to install a low-cost power plant capable of supplying electricity to a nearby residence.

II. MATERIALS AND METHODS

The equipment used for this work included the MNC from Cidade Velha, where metal structures were adapted to fix measuring devices such as the Pitot tube, manometers, and the turbine operation station. The turbine operation station consisted of a metal structure to which the researchers adapted each fully constructed turbine, the electric motor (Washing machine motor) or an electric generator (car alternator) that was part of our installation. The connection between the turbine and generator shafts was made using pulleys and a belt. Other equipment used were two manometers, a 25 frames/s video camera, a 12 Volt and 80 Ampere Tudor battery, a digital multimeter, a charge controller, a 12V to 220 V Inverter, the cables for connecting the equipment and transmitting energy to a nearby house.

This study explores the potential of MNCs as a source of energy from ocean waves. For this purpose, the researchers identified several of these infrastructures along the Coast of Santiago Island in Cabo Verde through an extensive field investigation. These MNCs were later classified based on criteria such as Type of Access, Location, Presence of Surface Cavities, Average Diameter of these Cavities, the Amount of Water Aspirated, and their Energetic Content to identify the most suitable ones for energy production (Monteiro and Sarmento, 2014).

The best MNC identified was then the target of several experimental tests to understand its operation characteristics. The elected MNC was then studied when equipped with four different Wells turbines having several rotor blade orientations. Each turbine was constructed using low-cost material available in our country.

To test the turbines the researchers built, they measured and recorded the total flow pressure and static pressure drop across them. These values were read by U-tube manometers and captured by a video camera at a rate of 25 frames per second.

Based on the instantaneous values of the manometric fluid heights, the maximum instantaneous velocities (V_{Amax}) at the centerline of the tube were calculated. This calculation was performed using Eq.1, which was derived from Bernoulli's equation applied along the central streamline of the tube, assuming an incompressible and steady flow for very short time intervals (the data sampling time). In Eq.1, Δh represents the vertical displacement of the manometric fluids, g = 9.81 m/s² is the gravitational acceleration, and ρ_{air} and ρ_{water} are, respectively, the densities of air and water (manometric fluid).

$$V_{Amax} = \sqrt{\frac{2\rho_{H_2O} g \Delta h}{\rho_{ar}}} \quad (1)$$

With values of the velocity at the centerline of the vertical tube and assuming a turbulent velocity profile for a circular tube, as defined by Eq.2 (White, 1991), the average velocity was calculated.

$$\frac{V(r)}{V_{Amax}} = \left(1 - \frac{r}{R_h}\right)^{\frac{1}{n}} \quad (2)$$

In the above equation, r represents the distance from the centerline of the tube to any point in the flow, and R_h is the hydraulic radius, since the tube has a rectangular geometry.

In Eq.2, n is generally a function of the Reynolds number. However, for this study, $n=7$ was used, as this power law provides a good description of the turbulent velocity profile (White, 1991). The hydraulic radius is defined by:

$$R_h = \frac{ab}{a+b} \quad (3)$$

where $a=30\ cm$ and $b=15\ cm$ are the dimensions of the cross-section of the vertical tube fixed to the cave orifice.

By definition, the average velocity is calculated as follows:

$$V_A = \frac{1}{A}\int_A V(r)\, dA = \frac{1}{\pi R_h^2}\int_0^{R_h} 2\pi V(r) r\, dr \quad (4)$$

By substituting the expression for $V(r)$ into the previous equation and solving the integral, the average flow velocity (V_A) is given by the following

http://dx.doi.org/10.21622/RESD.2024.10.2.1019

expression:

$$V_A = \frac{2n^2}{(2n+1)(n+1)} V_{Amax} \quad (5)$$

The volumetric flow rate of air passing through the cross-section of the duct, considered circular with hydraulic radius , R_h was calculated based on the average flow velocity using the following expression:

$$Q = \pi {R_h}^2 V_A \quad (6)$$

The power available for conversion by the turbo-generator group was calculated by the product of static pressure drop across the turbines and volumetric air flow rate through them, using the following equation:

$$P_{ar} = dpQ \quad (7)$$

In Eq.7 dp is the pressure drop across the turbine. The hydrodynamic efficiency of the turbine and the flow coefficient were calculated using the following equations:

$$\eta^* = \frac{P}{dpQ} \quad (8)$$

And

$$\varphi = \frac{V_A}{\omega R_{tip}} \quad (9)$$

In the equations above P and R_{tip} are, respectively, the mechanical power at the turbine shaft and the turbine tip radius.

The mechanical power P at the turbine shaft was determined using the relation $P=M\omega$, where the turbine torque $M=I(d\omega/dt)$. Here, ω is the angular velocity of the turbine shaft, and I is the moment of inertia of the turbo-generator set which was experimentally estimated in Lab to be equal to 145 g·m². The angular velocity of the turbine shaft was determined from the rotational speed of a tachometer shaft which was connected to the turbine shaft. The voltage signals from the tachometer were converted into turbine angular velocity using the tachometer calibration curve, which was determined in the lab. This calibration curve was then implemented in Arduino through C++ code, which converted the electrical signals from the tachometer into the turbine's angular velocity.

The term $(d\omega/dt) = (\omega_{i+1} - \omega_i) / \Delta t$ represents the angular acceleration of the turbine, where $i+1$ refers to the future time instant, i refers to the past instant, and $\Delta t = t_{i+1} - t_i$ is the corresponding time interval for sampling, which was 0.1 seconds for this study.

Finally, the excitation of the cave is highly dependent on tidal states and wave characteristics (López *et al.*, 2017 and Monteiro *et al.*, 2021). Therefore, comparing the performance of the cave when equipped with each Wells turbine was a very challenging task. However, by analyzing the tide charts for Santiago Island, available on the website tabuasdemarés.com, it became possible to select the best times to conduct experiments in the cave, allowing for this comparison. All the comparisons the researchers made between the performance of the different turbines studied in this work were realized under very similar tidal conditions. Next, they present the flowchart of the methodology used to carry out this work.

Volume 10, Issue 2, December 2024 - ISSN 2356-8569
http://dx.doi.org/10.21622/RESD.2024.10.2.1019

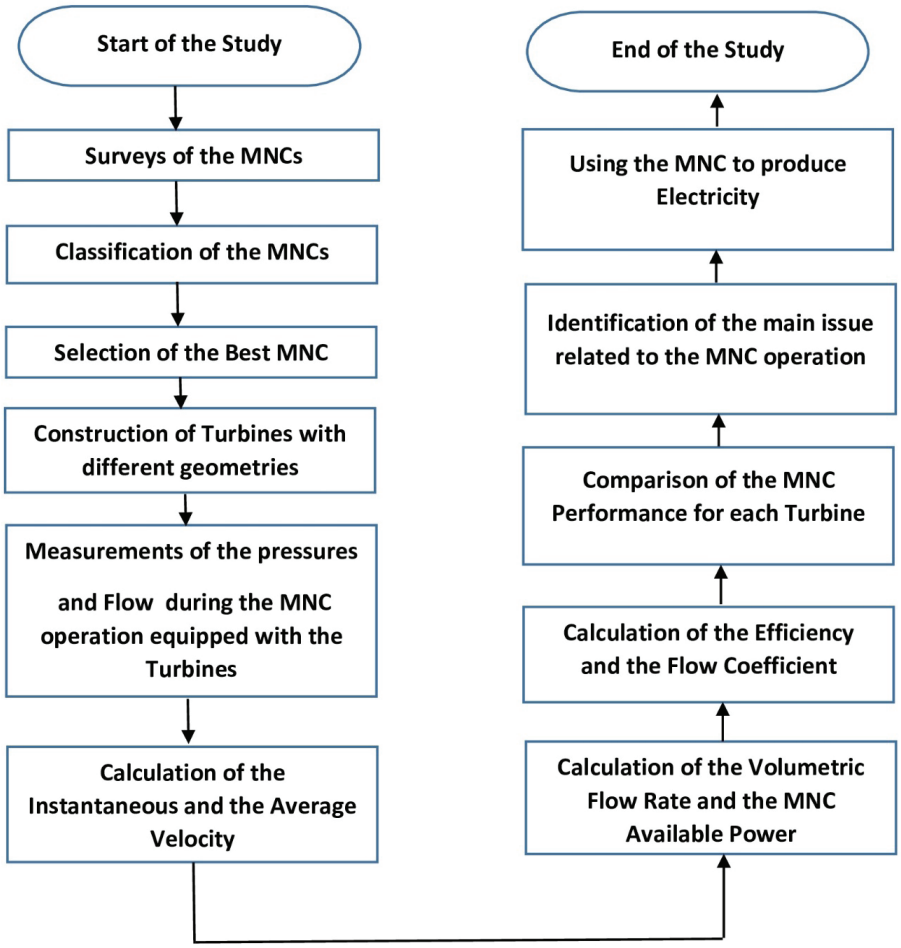

Fig. 2. The flowchart of the methodology

III. EXPERIMENTAL APPARATUS AND WELLS TURBINES DESIGN

The experimental setup the researchers built for the study of the cave equipped with the Wells turbine consists of a motor (model: *MCA 38/64-148/WHE1*) with an integrated tachometer to measure the rotational speed of its shaft, the turbine fixed to its workstation and connected to a vertical air duct, along with an Arduino and an Ethernet Shield board with a memory slot for data logging. The turbine shaft is directly coupled to a 16.8 cm diameter pulley, which connects to another 6 cm diameter pulley attached to the generator shaft. This setup results in a speed multiplication at the generator shaft by a factor of 2.63, corresponding to the ratio of the pulley diameters (Beer et al., 2013). The two pulleys are connected by a belt. The photograph of the experimental setup used to study the performance of the natural cave in Cidade Velha is shown in Fig. 3.

Fig. 3. Experimental setup to study the MNC production when equipped with the Wells turbine

In Fig. 3, one can also see a voltage rectifier that converts the tachometer voltage signal from 0 to 10 V AC into 0 to 5 V DC, which is compatible with the Arduino (Kuphaldt, 2006, 2009).

Volume 10, Issue 2, December 2024 - ISSN 2356-8569
http://dx.doi.org/10.21622/RESD.2024.10.2.1019

To size the Wells Turbine, which converts the cave pneumatic energy into useful mechanical energy, the researchers used data from previous studies that quantified the cave energy potential.

Based on the data from Table II, four turbines were built, each with a different rotor blade pitch angle (β). The steps involved in this process are described in detail below.

The performance of the MNC was analyzed when it was equipped with turbines having four different rotor blade inclinations which are β=0°, β=5°, β=10° and β=15°. These turbines were entirely built using materials available in Cabo Verde, as the study was conducted during the quarantine period due to the COVID-19 pandemic. Furthermore, with the disruptions of all flights and international transactions due to this pandemic, it became evident that the researchers need to start developing indigenous technologies and reduce their dependence on external markets for material and equipment supplies.

To build the turbines, the researchers used PCV tubes of different sizes, fiberglass mat, polyester resin, hardener, and catalyst (Fig. 4). They opted for PVC tubes due to their corrosion resistance and easy availability in Cabo Verde, as well as being more cost-effective.

Fig. 4. Materials used for constructing the Wells turbines

The turbine construction process was initiated by building its hubs and deflectors. The hubs were made from PVC tubes with a 200 mm diameter tube, cut into four pieces each measuring 4 cm in height (Fig. 5). These hubs were prepared using sandpaper and appropriate tools. Next, the PVC tubes were heated and transformed into PVC sheets (Fig. 5), which were moulded onto the 200 mm diameter tube orifice to form the deflectors, using a wind turbine deflector as a template (Fig. 5). The deflectors were then cut out and attached to the turbine hub using glue and screws (Fig. 5).

Fig. 5. Construction of the Wells turbine hubs and deflectors

To construct the turbine blades, the researchers began drawing them on a piece of cardboard (Fig. 6). This sketch was then transferred onto PVC sheets (Fig. 6), and subsequently cut out (Fig. 6). Additionally, NACA0021 profiles were drawn and cut to seal the ends of the blades (Fig. 6).

Fig. 6. Turbine blade surfaces and the NACA profiles

The turbine blades were shaped using heat, and their ends were sealed (Fig. 7). Finally, these blades were glued onto the hubs using special adhesives, respecting their inclination angles (Fig. 7).

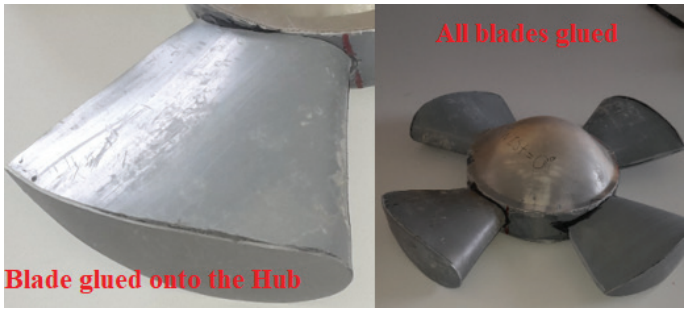

Fig. 7. The turbine blades were glued to the hubs

To fiber the turbines, precise mixtures of polyester resin, hardener, and catalyst were prepared in advance. The proportion of these elements in the mixture was carefully determined based on advice from professionals who work with these materials for boat construction (Fig. 8). This proportion was well calculated to achieve greater hardness and drying efficiency of the turbines.

Volume 10, Issue 2, December 2024 - ISSN 2356-8569
http://dx.doi.org/10.21622/RESD.2024.10.2.1019

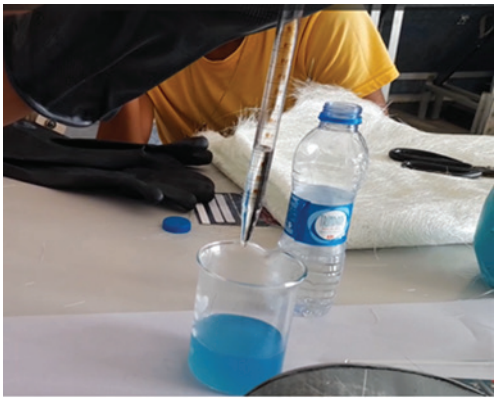

Fig. 8. Mixtures preparation for the fiberglassing of the turbine

Next, using a brush, several layers of fiberglass were made to achieve greater hardness and to produce more resistant turbines (Fig. 9). Then, the turbines were subjected to a natural drying process and polishment using sandpaper (Fig. 9). Using a lathe, all turbines were drilled at its centre to accommodate their respective transmission shafts. A finishing process was carried out to improve the smoothness and, finally, their surface painting was done.

Fig. 9. Fiberglassing and finishing of the Wells turbines

IV. RESULTS AND DISCUSSION

In the following, the researchers present the main results of this work.

A. Characterization of MNCs Founded Around Santiago Island

To assess the energy performance of MNCs able to be used in the future for electricity production purposes, they were, in advance, classified taking into account a set of criteria that has been mentioned before and explained by Monteiro *et al.* (2014). Due to a lack of funding, it was not possible to extend this study field to all Cabo Verde Islands. Thus, the largest island of the country, Santiago Island, was chosen for the present study. Around the Island, a set of nine most relevant MNCs was found. These MNCs, as well as their respective locations, are shown in Figs 10 to 19.

According to Monteiro *et al.* (2019), the MNCs located to the south of Santiago Island are more promising since they are subject to more energetic waves. As can be seen in Fig. 19, the MNCs of Porto Mosquito, Cidade Velha, Farol and Palmarejo stand out in this context. However, the remaining MNCs, although they may be subject to less energetic waves, may be of interest, taking into account the previous selection criteria.

Fig. 10. Natural Cave - Farol

Fig. 11. Natural Cave - Porto Mosquito

Volume 10, Issue 2, December 2024 - ISSN 2356-8569
http://dx.doi.org/10.21622/RESD.2024.10.2.1019

Fig. 12. Natural Cave – Rincão

Fig. 13. Natural Cave – Palmarejo

Fig. 14. Natural Cave - Praia-Baixo

Fig. 15. Natural Cave – Cidade Velha

Fig. 16. Natural Cave - Ponta Preta

Fig. 17. Natural Cave - Redondo

Volume 10, Issue 2, December 2024 - ISSN 2356-8569
http://dx.doi.org/10.21622/RESD.2024.10.2.1019

Fig. 18. Natural Cave - Cobon-de-Lacha-Monte

Fig. 19. Location of MNCs around Santiago Island

According to the predefined selection criteria, the most interesting MNCs must have a superficial cavity, not too large (to facilitate the adaptation of measuring equipment), with little or no water in the jet and be close enough to the housing. The characteristics of each MNC found during this study field are shown in Table III. In this table, the nine MNCs found around Santiago Island are listed in decreasing order of importance, taking into account the previously used selection criteria. Therefore, analysing each MNC shown in this table, it is possible to note that the ones located at Cidade Velha and Praia-Baixo are the most interesting since they fully meet the criteria requirements.

TABLE III
CHARACTERIZATION OF MNCS.

Region	Cavity	Shape	Access	Location (m)	Average Diameter (m)	Amount of the water in the jet	Ranking
Cidade Velha	With cavity	Rounded	Easily (by sea and land)	Very close (130)	0.5	none	1
Praia-Baixo	With cavity	Rounded	Easily (by sea and land)	Very close (850)	0.6	none	2
Porto Mosquito	With cavity	Rounded	Easily (by sea and land)	Very close (90)	0.3	A few	3
Ponta Preta	Double cavity	Rounded	Easily (by sea and land)	Very close	0.5-0.8	A few	4
Redondo	Without cavity (with cracks)	Elongated	Easily (by sea and land)	Very close	-	A few	5
Cobon de Lacha Monte	Without cavity (with cracks)	Elongated	Easily (by sea and land)	Very close	-	A few	6
Palmarejo	With cavity	Elongated	Easily (by sea and land)	Very close (350)	-	A lot	7
Rincão	With cavity	Elongated	Easily (by sea and land)	Very close (900)	-	A lot	8
Farol Maria Pia	With cavity	Rounded	Easily (by sea and land)	Very close (120)	0.8	A lot	9

Volume 10, Issue 2, December 2024 - ISSN 2356-8569
http://dx.doi.org/10.21622/RESD.2024.10.2.1019

Any of these MNCs could be subjected to the experimental study. However, due to budget constraints, the one located at Cidade Velha was chosen to be the target of a more deeply study to evaluate its energy performance. Another reason that justifies this choice is related to the patrimonial and touristic nature of the city where the MNC is located, which may facilitate access to the funds to implement hereafter a wave energy plant based on these natural infrastructures. Further, this kind of infrastructure may be very well incorporated into a project of tourist attractiveness for Cidade Velha city.

The MNC located at Cidade Velha was visited three times, during which the researchers qualitatively evaluated, in locus, the energy associated with its operation. Such evaluation showed that this MNC presents good conditions for carrying out the experimental study.

As one can see in the following picture, the cave orifice was sealed by a big rock. This was done by the local inhabitants as a way of mitigating the noise that was associated with its operation. After removing the aforementioned stone, it was verified that the orifice of this MNC has a geometry almost rectangular, with dimensions of 15 cm×30 cm and is located around 50 cm below the shore surface.

Fig. 20. Cidade Velha MNC (obstructed by stones)

According to Fig. 20, the entrance to the target MNC is tapered, which increases the wave height at its opening and, consequently, the energy available during its excitation by incident waves.

B. *The Characteristic Curves of Turbines*

Following the method previously described to measure the pressure drop in the turbines ($H_t[cmH_2O]$) and calculate the airflow through them (Q), it was possible to create the relationship $H_t=f(Q)$ for each turbine, forming their characteristic curves. Fig. 21 shows these curves for each turbine studied. The lines in the graph are linear (Fig. 21 a) and quadratic (Fig.21 b) approximations of the experimental data.

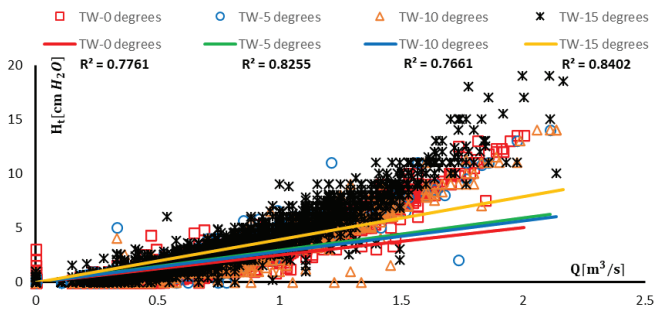

a-Linear

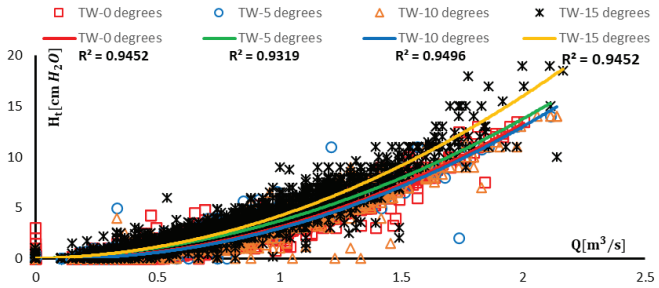

b-Quadratic

Fig. 21. The characteristics curves of the Wells turbines

Despite the significant data dispersion, the linear approximation curves (Fig. 21 - a) have a determination coefficient (R^2) above 75%, which is quite satisfactory, especially in real measurement environments, as in this study. This means that the linear model fits well with the experimental data, indicating that more than 75% of the variation in the pressure drop through the turbines is explained by the airflow through them. However, it is evident that for higher flow rates, the turbines tend to exhibit a non-linear relationship between H_t and Q. Indeed, for high flow rates, the characteristic curves of the turbines seem to follow a quadratic behavior (Fig. 21 - b). This behavior can be, at least partially, explained by the boundary layer separation on the rotor blades of the turbine. Using a quadratic approximation of the characteristic curve data, we obtained determination coefficients above 93%, suggesting that this approximation is closer to the experimental data compared to the linear one. As the flow increases, the deviation between the linear and quadratic approximation becomes more pronounced. Comparing the linear and quadratic approximations,

Volume 10, Issue 2, December 2024 - ISSN 2356-8569
http://dx.doi.org/10.21622/RESD.2024.10.2.1019

it was possible to verify that this deviation is more significant when $Q>0.9\ m^3/s$. Another observation from Fig. 21 is that the characteristic curve of the turbine with β=10° is below that of the turbine with β=5°. This result was unexpected and may be related to data approximation errors. Later in this work, the researchers clarify this by comparing the shaft power for these two turbines.

C. *MNC Production*

Fig. 22 shows the temporal evolution of the shaft power of the turbines with blade angles β=0° (Fig. 22a) and β=15° (Fig. 22b) during the first and second high tides. These graphs do not reveal a clear trend in the extracted power values over time, nor do they show a significant influence of the different tidal states on this operational parameter of the cave. This was expected since the tidal conditions during the measurements were very similar.

However, when analyzing the data from the operation of the cave equipped with β=0° blade angle turbine, two unusual observations were identified. These points appeared in both the first and second high tides and were considered outliers. By examining the time series, it was found that these outliers occurred due to a sudden acceleration of the turbine, starting from an almost stationary state. Although these outliers are considered authentic, they were not deemed relevant to the conclusions of this study.

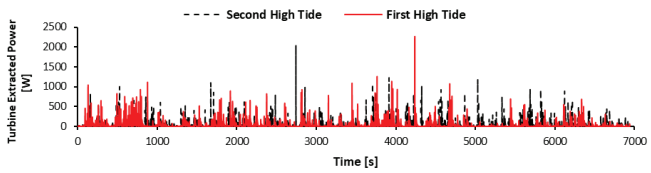

(a)

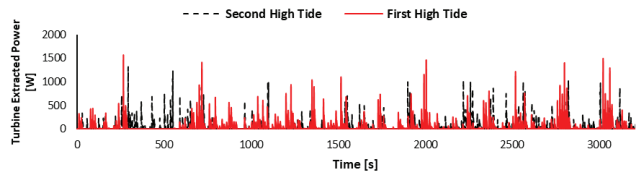

(b)

Fig. 22. Turbine extracted power as a function of time: a- for β=0° and b- for β=15°

Another aspect that stands out in the graphs of Fig. 22 is the display of significantly different values of power at the turbine shaft over time. This variation has a direct implication on the turbine efficiency and the design of the electric generator to converting the shaft power into electricity. Furthermore, disregarding both outliers mentioned before, it can be observed that the values of the power obtained with the turbine at β=15° reached higher levels (close to 1800 W) compared to those of the turbine at β=0°, which were around 1500 W. This suggests that the turbine at β=15° adapts better to the operational conditions of the cave compared to the turbine at β=0°. This conclusion is reinforced by the analysis of the graphs in Fig. 23, which compare the performance of the cave equipped with each of these turbines over time.

Thus, Fig. 23 compares the temporal values of power extracted by the turbine with β=0° and β=15° over 55.5 minutes of cave operation, for the first low tide (Fig. 23 a) and second low tide (Fig. 23 b). The graphs clearly show that the turbine with β=15° generally achieves higher power levels during the observed period. This suggests that the turbine with β=15° performs better in the cave operation compared to the turbine with β=0°. Furthermore, upon closely analyzing Fig. 23, it was observed that the difference between the shaft power values of the two turbines is more pronounced during the first tide than during the second.

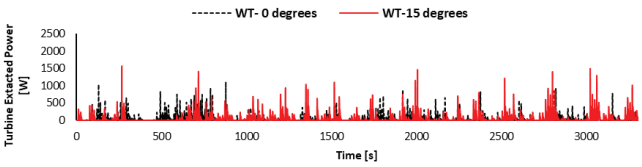

(a)

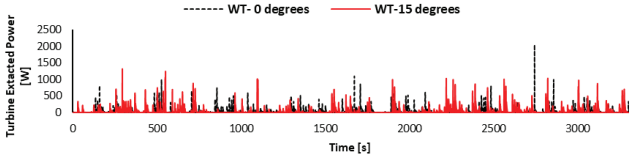

(b)

Fig. 23. Comparison of Turbines: a-first high tide and b-second high tide

The maximum power values achieved were 1255 *kW*, 1553 *kW*, 1399 *kW*, and 464 *kW*, respectively, for turbines at 0°, 15°, 10°, and 5° of rotor blade inclination. The rotation speeds at which these powers were

Volume 10, Issue 2, December 2024 - ISSN 2356-8569
http://dx.doi.org/10.21622/RESD.2024.10.2.1019

recorded were 1193 *rpm*, 1101 *rpm*, 573 *rpm*, and 490 *rpm*, respectively. The maximum rotation speeds recorded were 1217 *rpm* (for 0°, 15° and 10°) and 912 *rpm* for 5° of blade inclination. This means that the zero-degree turbine needs to rotate at around 1193 revolutions per minute to produce maximum power. This can be achieved using an appropriate control system. These power values place the turbine with a 15-degree blade inclination in the lead, followed by the turbines with 0, 10, and 5 degrees of inclination, with the latter being the least recommended.

From the analysis of the characteristic curves of the two best turbines (Fig. 21), the researchers observed that the turbine with β=15° produced higher pressure drop values (H_t) than the turbine with a β=0° inclination for very similar flow rates. Therefore, it was expected that the turbine with β=15° would produce higher power compared to the turbine with β=0°. In fact, under similar operating conditions, the turbine with a 15° inclination produced an average of 52 W compared to the turbine with β=0°, which produced around 47 W of shaft power. Additionally, during this same operating period of the cave, the turbine with β=15° exhibited an accumulated shaft power of 428.66 kW compared to 391.87 kW for the turbine with β=0°. This confirmed that the turbine with β=15° was better adapted to the operating conditions of the cave during which the test was conducted. In other words, there was a 9% increase in the accumulated power value for the MNC using β=15° rotor blade turbine. Furthermore, as shown by the trend lines of these two turbines that tend to diverge with increasing flow rate (Fig. 21), it was expected that the difference in the adaptation of these two turbines to the extreme operating conditions of the cave would become even more pronounced.

Table IV shows the operational characteristics of both turbines under analysis (β=15° and β=0°) over 55.5 minutes of cave operation. According to the values shown, although the turbine with β=15° is better suited to the MNC, it remained inoperative for a longer period (20.18 minutes) than the turbine with zero degrees (17 minutes). In other words, the turbine with β=15° had 475 more stops than the turbine with β=0°. Additionally, it was observed on-site that the turbine with β=15° faced significant difficulties in starting and maintaining operation when the cave energy content varied from low to moderate, especially during MNC suction. All of this impacted the amount of energy produced by the MNC when equipped with the turbine with β=15°. Therefore, despite all these operational constraints, the turbine with β=15° still exhibited higher average and accumulated power, further reinforcing its better adaptability to cave operation.

TABLE IV
OPERATIONAL CHARACTERISTICS OF THE TURBINES DURING 55.5 MINUTES OF CAVE OPERATION.

Wells Turbines	Number of Turbine Shutdowns	Number of Turbine Operations	Turbine Downtime Periods
β=0°	2540	5757	17 minutes
β=15°	3016	5281	20.2 minutes

As a result, based on the behaviour of the turbines studied, it may be possible to improve cave production by adapting an intelligent control system for the turbine blade angles and adjusting them according to the MNC excitation conditions. In other words, during the start-up and deceleration moments of the turbine, the system should fix the turbine rotor blades at β=0° to facilitate start-up, delay its stop, and reduce the number of stops. During full turbine operation, the system should fix the blades at β=15°. However, it is important to remember that changing the inclination of the turbine blades affects the system damping coefficient, which can positively or negatively influence the hydrodynamic efficiency of the MNC (López *et al.*, 2017).

Fig. 24 shows the turbine shaft power as a function of airflow, for the two best turbines found. Despite the large data dispersion, it is possible to observe from this graph a clear trend of decreasing shaft power in both turbines as the flow rate increases. This indicates that the turbines tend to lose efficiency at higher flow rates. This loss of efficiency is associated with the separation of the boundary layer on the turbine blades.

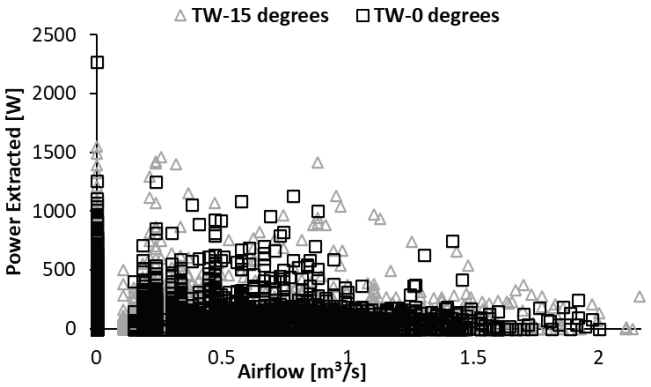

Fig. 24. Power extracted by turbines

Volume 10, Issue 2, December 2024 - ISSN 2356-8569
http://dx.doi.org/10.21622/RESD.2024.10.2.1019

It is also noticeable again that the shaft power values for the turbine with blades inclined at β =15° are generally higher than those for the turbine with blades at β = 0° orientation and this behaviour persists even at higher flow rates. The increase in shaft power when using the turbine with β =15°may be related to a delayed separation of the boundary layer on its blades, compared to what happens with the turbine with β = 0° orientation.

Another interesting observation from Fig. 24 is that the turbine generated power at the shaft even without airflow. This happened when the turbine was in motion and no longer driven by the MNC, maintaining its movement due to inertia. This behaviour occurred whenever the energy from the MNC was insufficient to change the turbine's movement.

D. Hysteretic Behavior of the MNC with Wells Turbine

Our studies at the MNC in Cidade Velha have shown that it exhibited hysteresis behaviour, even when not equipped with the Wells turbine. This could be explained by several known factors that can cause hysteresis in the studied system, such as air compressibility in the pneumatic chamber, wave swelling, and the delay between pressure sensor measurements used in our setup. However, to identify which of these factors contributes most to the hysteresis observed in the MNC, further studies are needed.

The two pressure sensors in the experimental setup were positioned along the vertical duct, 1.5 m apart (Fig. 25). This probably caused a time delay between the measurements taken by both probes. Thus, when a flow passes through the total pressure sensor, the static pressure sensor is affected by the flow that passed through the total pressure sensor moments before. Because of this time lag, the power available in the cave and the power at the turbine shaft were also out of sync. As a result, this caused significant errors in assessing the cave efficiency. This effect can be minimized by selecting equipment with appropriate response times for the phenomenon under analysis and positioning them as closely as possible.

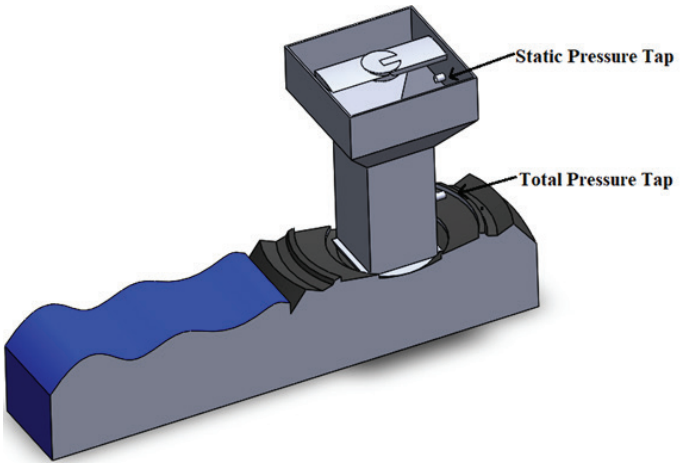

Fig. 25. Total and static pressure taps

To highlight the contribution of turbine dynamics to the hysteresis phenomenon, the researchers present Fig. 26, which shows the evolution of the turbine efficiency with 15-degree inclined blades as a function of the flow coefficient, operating in two high tide states. As indicated in the graph, there is a rapid decrease in turbine efficiency as the flow coefficient increases, which points to the turbine difficulty in converting energy, especially during moments when the cave exhibits high energy levels. This reinforces the observations made in Fig. 24.

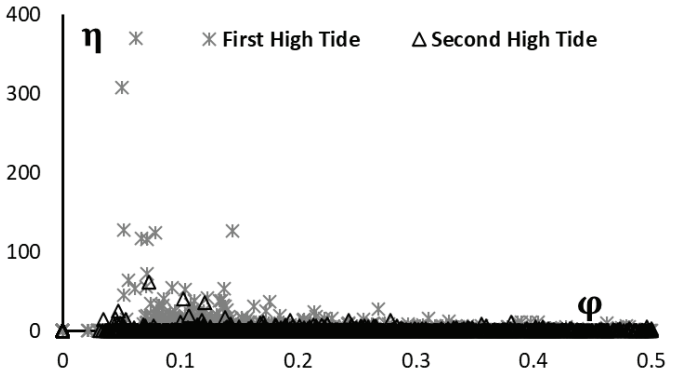

Fig. 26. Turbine efficiency

Disregarding some extremely high-efficiency values recorded during the turbine test in the first high tide, it is possible to observe that the turbine efficiency, at certain moments, exceeded 50, suggesting that the power at the turbine shaft was about 50 times greater than the power available in the cave. This behaviour is not unexpected, as in such situations, the turbine

Volume 10, Issue 2, December 2024 - ISSN 2356-8569
http://dx.doi.org/10.21622/RESD.2024.10.2.1019

stored energy from previous excitations, causing the power at the shaft to be significantly higher than the power available in the MNC. Therefore, this study highlighted that turbine dynamics is a crucial parameter in assessing the MNC performance. Furthermore, the turbine efficiency does not serve as the best indicator of its performance in an MNC, as it is subject to significant errors.

The hysteresis caused by the inertia of the turbine, the researchers believe, cannot be eliminated and will always be present in the data. For this reason, they recommend that the assessment of the performance of the MNC or similar devices be based on the shaft power values of the turbine.

E. Experimental Power Plant from the Cidade Velha MNC

One of the most important stages of this work was the implementation of a low-cost experimental power plant from the Cidade Velha MNC to supply electricity to a house located nearby.

To make the power plant, the researchers used low-cost equipment which was a Wells turbine, a car alternator (generator) which requires pre-excitation to produce voltage, a 12V battery, a 12V DC voltage inverter, a battery charge controller, a switch, a relay, and all the wiring for connecting this equipment and transmitting electricity from the plant to the target house.

All equipment used in the power plant was tested in the Lab before being installed in the MNC (Fig. 27).

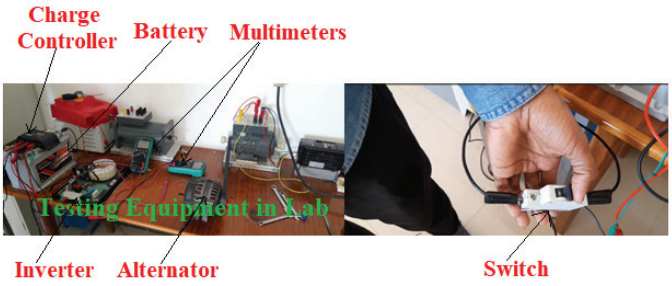

Fig. 27. Testing the Power plant equipment in the Lab

After assembling all the equipment, the generator was then triggered with the help of a drill. The excitation of the alternator is switched on using the switch shown in Fig. 27. Thus, when the alternator starts producing voltage, which is monitored using a multimeter, the excitation is turned off, and the alternator continues to produce voltage. The voltage was then sent to the battery. In turn, the battery activated the voltage inverter, which converted the 12 V (DC) voltage from the battery into 220 V (AC) which is the voltage of our electric network (Fig. 28).

Fig. 28. Testing the Inverter

After installing the alternator at the turbine operation station, the turbo-generator set fixed at the turbine operation station was connected to the vertical MNC tube. The alternator was then excited by the battery of the installation that constituted the storage element of energy produced by the power plant. The battery charge was monitored by a Steca controller, model 2020, which then sends energy to an 800 W Fronius voltage inverter. The output of the inverter is directly connected to the target house's electrical panel. Energy transmission from the inverter to the house was done using a 50 m-long cable (Fig. 29).

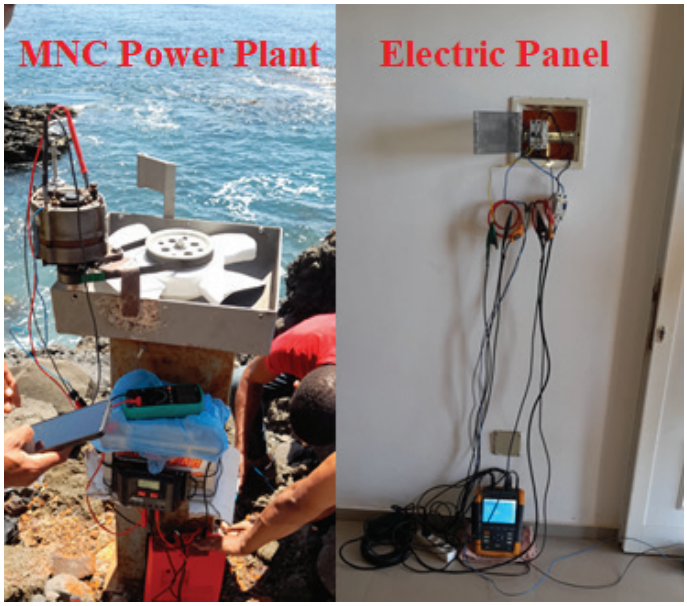

Fig. 29. MNC Power Plant connected to the electrical panel

F. The Experimental Power Plant Monitoring: The Lesson Learned

This study showed that the experimental power plant based on the Cidade Velha MNC can

Volume 10, Issue 2, December 2024 - ISSN 2356-8569
http://dx.doi.org/10.21622/RESD.2024.10.2.1019

support the consumption of nine 5 W LED bulbs, a refrigerator, and other devices (such as mobile phone chargers and computers). However, due to the characteristics of the inverter used, it was not possible to start the plasma television existing in the house.

The monitoring of the plant occurred over 24 hours, covering two high tides. During these operating periods, the battery voltages and the alternator output were constantly monitored. Unfortunately, it was noted that the power plant was unable to replenish the energy consumed from the battery by the electrical consumption equipment in the target house. This was because the alternator, that charges the battery, is not suitable for this application, as it is designed to generate voltage at high rotational speeds. The problem arose when the alternator, once excited, exhibited a very high rotation inertia, resulting in a high starting torque. Therefore, there were few moments during the MNC operation when the turbine reached speeds required by the alternator to start producing voltage to charge the battery.

According to the test carried out in the Lab, it is possible to disconnect the excitation of the alternator and reduce its rotational inertia. It can be done when the alternator rotation speed is close to its nominal value. However, to do this, the researchers need to associate the alternator operation with a control system able to connect and disconnect its excitation according to its rotational speed.

G. Structural Problems of Constructed Wells Turbines

The turbines have encountered several issues, especially at high rotational speeds. Vibrations, noise, the breaking of the blade tips, and the loosening of the bolts securing them to the operation station were some of the critical issues we identified. The researchers believe that noise and vibrations are linked to potential inaccuracies during turbine construction, causing unbalanced mass problems (Lees, 2020). At high turbine speeds, the vibrations caused the blades to touch the turbine station, releasing sparks and loosening the bolts connecting the turbine to its operating station, as well as to the vertical air duct. Additionally, when the turbine rotational speed reached very high values, the centrifugal force on the blades was so high that it caused the breaking of their ends, resulting in significant blasts (Fig. 30).

Fig. 30. Blade cap destroyed by centrifugal force

These incidents have raised some issues about the safety of the proposed installation, which need to be addressed. All these issues have made it clear that there is a need to introduce improvements to enhance its safety. To improve safety and extend the lifespan of the proposed installation, it is necessary to enhance the precision of the turbine construction, eliminating possible asymmetries that could cause balance issues, especially at high rotational speeds. The researchers will also strengthen the turbine structure by adding extra layers of fibreglass to its surfaces for increased durability. Additionally, they will minimize connection components that may loosen due to vibrations. One solution for this is to connect the turbine directly to the generator shaft, eliminating motion transmission elements such as belts and pulleys. Finally, the researchers will implement protective structures around the installation to prevent any projected parts from posing a risk to the safety of nearby individuals.

H. Natural Caves vs. Artificial OWC Devices

Exploring natural marine caves for electricity production is an innovative idea, still in its early stages. At this point in this study, the main goal of the researchers was to assess the technical feasibility of using these caves. In other words, the researchers focused on analyzing the energy potential of the caves and their behaviour in response to changes in sea conditions. Therefore, comparing natural caves to more advanced technologies would be premature and inappropriate at this stage, and they do not intend to do so at this point in the research. However, it is anticipated that using these caves could lead to reduced construction costs compared

to artificial coastal OWC plants, especially regarding the construction of the pneumatic chamber, which in the case of caves is naturally formed by the rock formations.

Natural caves present certain inefficiencies due to their morphology, which significantly reduces their overall energy conversion efficiency. The researchers believe that the efficiency of these natural structures will be considerably lower than that of equivalent artificial infrastructures. These inefficiencies are related to the irregular entrance of the caves and the presence of rocks typically found along the airflow path. Additionally, in the specific case of the cave studied, there are large rocks in front of the entrance, which cause waves to break before reaching the cave, significantly reducing their energy.

Another challenge related to the use of natural caves is their low energy generation capacity. A significant concentration of nearby natural caves would be necessary for their use to be technically and financially viable.

This issue does not arise with artificial OWC plants, as they are designed to operate with maximum efficiency, considering the wave conditions at the installation site. In the case of caves, the researchers are limited to the existing natural formations, along with all the physical constraints that impact their energy extraction efficiency.

Another important aspect related to the investment cost of an MNC power plant is the representation of civil costs, which account for about 27% of the total investment. This figure indicates a significant reduction in civil costs compared to the 80% associated with an artificial OWC (Oscillating Water Column) power plant.

I. Analysis of Weaknesses and Inaccuracies

This study faced several limitations, primarily budgetary and circumstantial, as a significant part of the work was carried out during the quarantine period imposed by the COVID-19 pandemic. Additionally, there were physical constraints due to the morphology of the natural cave being studied. These challenges, along with the harsh marine environment, dictated the choice of accessories and equipment adapted to the cave's orifice to carry out the necessary measurements to assess its energy potential.

As a result, the researchers recognize that the equipment and methodologies used to measure the physical parameters of the cave operation were not the most appropriate, leading to some weaknesses in this study. One of these weaknesses is related to the geometry and dimensions of the vertical tube connected to the cave orifice, which also served as support for the turbine station. The rectangular geometry and the cross-sectional dimensions of this tube were determined by the natural shape of the cave orifice, which led to greater energy losses in the airflow compared to the expected if we had used a circular tube.

Another issue associated with the use of this vertical tube is its length. To calculate the airflow exiting the cave, it was assumed that the flow inside the tube was turbulent and rough, which would require a longer tube. However, the tube used is only 1.5 meters long, which is insufficient to validate this assumption. Nevertheless, the researchers acknowledge that it would be physically impractical to use a tube of the necessary length to meet this condition.

The harsh marine environment also required the use of robust equipment for the measurements, which introduced some gaps in the results. To measure the pressures, U-tube manometers were built, and a Pitot tube was used. The Pitot tube, employed to measure the total pressure at the centre of the vertical air tube, should have been calibrated beforehand to correct possible inaccuracies. Additionally, the real-time measurement of the manometric fluid levels, using video cameras, introduced parallax errors in our measurements.

Finally, the turbine geometry, designed based on the cave operating conditions, required that the station be larger than the supporting vertical tube. This caused the airflow to decelerate as it entered the turbine station, negatively affecting its efficiency. The researchers believe this is one of the main limitations of this study, which should be addressed in future work.

It is important to emphasize that treating the rectangular cross-section tube as an equivalent circular cross-section tube using the concept of hydraulic radius also introduces inaccuracies in determining the flow parameters. However, for

turbulent flow (Reynolds number, Re > 2300), the maximum magnitude of this error is expected not to exceed 12%, depending on the parameter being calculated (Frate et al., 2015). If the flow is in a laminar regime, the relative error will be higher, ranging from 11% to 23%, according to the same authors. The approximation of the turbulent velocity profile is another source of inaccuracy in the approach used to determine the flow velocity. There are two distinct flow regions inside the air duct: the entrance region and the fully developed flow region (Oliveira and Lopes, 2012). The approximation of the turbulent velocity profile is valid for tube lengths greater than the entrance length, beyond which the velocity no longer depends on the longitudinal coordinate (in the direction of the flow).

Additionally, the maximum relative errors associated with measuring flow velocity, static pressure, and dynamic pressure were estimated due to the use of U-tube manometers to assess these operational parameters of the cave. The errors observed were 8.2%, 16.8%, and 16.6%, respectively. These levels of error are quite acceptable for real-world measurements, as was the case in this study.

J. Preliminary Cost Analysis

The MNCs vary widely in terms of shape, location, and the energy they can extract from waves. All these factors can directly influence the cost of using these structures for energy generation, making an accurate cost analysis challenging. Nevertheless, in table V, the researchers provide the main cost estimates for certain aspects and accessories related to the implementation of MNC in Cidade Velha (1 kW). The total investment cost was approximately $2,137 per kW.

TABLE V
SOME INDICATIVE COSTS FOR A 1 *KW* MNC.

Interventions/Accessories	Estimated cost ($)
Construction and adaptation of the metallic structure into the cave orifice	468
Cabin for electric and electronic equipment	100
Mechanic, electrical and electronic equipment	1319
Installation	150
Logistic	100
Total	2,137

It is important to emphasize that the costs presented in the previous table are merely indicative and may vary significantly from one cave to another, as each cave has unique characteristics and requires specific interventions to be used as an energy production infrastructure. As discussed earlier in this study, the cave analyzed showed a need for further interventions in various aspects to achieve improvements before it can be used as a wave energy plant. All these additional interventions will increase the total cost of using it as a wave energy source, meaning that the final cost will certainly be higher than shown in the previous table

Anyway, the current total cost shown in the previous table is less than half of the total capital cost of the wave farm, which is projected at $4,509.68 per kW according to the International Energy Agency (IEA) for the year 2021. The same source forecasts that this cost will decrease to about $139.05 per kW by the year 2050 (IEA, 2021). This indicates that in less than 27 years, the capital cost of an artificial wave power plant is expected to become comparable to the current cost of MNC.

Another important aspect related to the investment cost of an MNC power plant is the representation of civil costs, which account for about 27% of the total investment (Table V). This indicates a significant reduction in civil costs compared to the 80% associated with an artificial OWC (Oscillating Water Column) power plant. However, it is still quite premature to consider this reduction in construction costs as definitive, and it is expected that they will increase, taking into account the planned improvements to the cave in the future

V. CONCLUSION AND FUTURE WORK

This paper summarizes the main results achieved through conducting several tests on the Cidade Velha MNC equipped with four different Wells turbines fully constructed during this work. Each Wells turbine presents a different blade orientation. All the details regarding the construction of these turbines, including the materials used, have been presented in this work. Additionally, it presents the attempt to use this natural infrastructure (MNC) to power a house with electricity.

The numerous studies conducted on the Cidade Velha MNC yielded a set of pertinent real-world data that are crucial for a better understanding of the behaviour of this type of energy infrastructure. These real data are interesting for designing MNC (OWC) and to understand better its behaviour.

Volume 10, Issue 2, December 2024 - ISSN 2356-8569
http://dx.doi.org/10.21622/RESD.2024.10.2.1019

All the characteristic curves of the turbines studied were determined in the real operational environment of the cave. According to the reached results, these curves show a linear trend, particularly with a determination coefficient above 75%. However, at higher flow rates, these curves seem to exhibit a non-linear behaviour that may be due to boundary layer separation on the turbine blades. The quadratic approximations of the experimental data fit better than the linear ones as they presented higher determination coefficient values (above 93%).

The reached results indicate that the blade angle of the turbine has a significant impact on cave production. In this context, the highest cave productions of 2044 W and 2266 W were achieved when a turbine with blades inclined at an angle of β=0° was used, operating respectively at 717 rpm and 755 rpm. However, these power values were considered outliers and, therefore, were not deemed relevant.

The turbines with β=15° and β=0° showed better performance during high-energy moments in the cave, while the turbine with β=0° proved to be less suitable for these situations. In fact, in 55.5 minutes of cave operation equipped with each of these two best turbines, the turbine with β=15° exhibited an average power of 52 W and a total accumulated power of 428.66 kW, compared to, respectively, 47 W and 391.87 kW for the turbine with β=0°. Additionally, the turbine with β=15° encountered more difficulties in starting and had a higher number of stops during the 55.5 minutes of operation. In fact, during this period of cave operation, the turbine with β=15° recorded 475 more stops than those exhibited by the turbine with β=0°. In other words, the turbine with β=15° was inoperative for about 8 minutes longer compared to the cave operation scenario with the turbine of β=0°. Despite all these disadvantages, the turbine with β=15° converted more energy than any of the other turbines studied.

Turbines with blade inclinations of β=15° and β=0° reached peak efficiencies of 369 and 273.8, respectively. However, these high efficiencies were impacted by the turbines inertial effects and the hysteresis experienced by the natural cave, as shown by the given data.

The turbines the researchers constructed revealed issues with vibration, noise, and structural nature, especially at high rotation speeds. These problems raised concerns about the operational safety of the MNC and were related to manufacturing inaccuracies in the turbines. At high speeds, worrying situations such as the disintegration of blade tips and loosening of bolted connections due to vibrations in the installation have occurred. When spinning at high speeds, the turbine exhibited imbalances that caused its blade tips to occasionally strike the workstation, resulting in sparks. All these situations highlighted the need for substantial improvements in both turbine construction and the overall power plant installation.

The MNC showed hysteresis behaviour. An important source of hysteresis in the studied MNC when equipped with the Wells turbine was the turbine inertial effect, which introduced significant errors in assessing the system performance. For this reason, the researchers recommend that turbine performance be assessed based on its shaft power rather than its efficiencies.

The MNC supplied electricity to the target house. The MNC power plant was able to ensure the consumption of nine 5 W LED bulbs, a refrigerator, and other devices (such as mobile phone chargers and computers). However, the power plant revealed significant challenges in replenishing energy in the battery. The main reason for this was related to the generator used in the power plant. It required high rotational speeds to produce voltage, only after pre-excitation. The pre-excitation of the generator increased its rotational inertia, leading to difficulties in starting the turbine and achieving the nominal rotation required to produce voltage.

Numerous aspects of the MNC can be enhanced to enable it to be tested again as a source of electricity for the chosen residence.

For future work, the researchers recommend improving the construction of the turbine to ensure the necessary symmetry, to reduce vibrations that propagate throughout the installation, causing structural and safety issues. It is also essential to reinforce the turbine structure to prevent its disintegration at high rotational speeds. They suggest repositioning the measurement probes to reduce the time lag between readings, which will help minimize the occurrence of hysteresis. Another important recommendation of this work is to measure and isolate the contributions of the capacitive effect of the cave and the measurement equipment on the occurrence of hysteresis in the system. This will help clarify even more the

influence of the turbine's inertial effect on the appearance of hysteresis.

Additionally, building a variable-geometry turbine (with adjustable rotor blade pitch) and conducting a deeper study on the impact of turbine geometry on both hydrodynamic and aerodynamic performance would be beneficial. Furthermore, it is recommended to thoroughly analyze the turbine start-up capacity and downtime about the blade pitch angle.

The study reinforces the requirement for a suitable generator and inverter for the power plant. The most commonly used generator type for this application has been the asynchronous one, directly connected to the turbine shaft. The researchers are working on a project aimed at designing and constructing an asynchronous generator for the Cidade Velha power plant. The experimental setup they use to study the energy profile of the MNC can be improved in several ways. They will increase the diameter of the cave orifice and replace the vertical conduit with a circular pipe, reducing flow losses. Additionally, they will ensure that the diameter of the turbine section is smaller than that of the vertical circular pipe that supports it, to accelerate the flow as it enters the turbine section, thereby improving its performance.

Additionally, two large rocks in front of the MNC cause the waves to break before reaching the entrance, reducing their energy. The researchers plan to remove these rocks in the future to allow the waves to reach the MNC entrance with more energy.

Several rocks at the MNCs orifice exit significantly increase the energy loss in the airflow. By removing these rocks, the cave will provide more energy to the turbine.

Finally, although the current estimated total cost for implementing an electricity generation plant using the cave in Cidade Velha is significantly lower than that estimated for artificial wave energy plants, and there has been a substantial reduction in the share of construction costs in the total cost of the plant, it is expected that both will ultimately be higher, considering the interventions planned for the future to make the Cidade Velha plant more viable and secure.

Acknowledgements

Special thanks go to the United Nations Development Programme – PNUD and to the Cabo Verde Ministry of Education for financing the presented study. The researchers direct many thanks to all colleague and Energy Lab monitors for their valuable contribution to the realization of this work.

References

[1] A. Barua and M. Salauddin Rasel, "Advances and challenges in ocean wave energy harvesting," *Sustainable Energy Technologies and Assessments*, vol. 61, p. 103599, Jan. 2024, doi: 10.1016/j.seta.2023.103599.

[2] A. F. de O. Falcão, "Wave energy utilization: A review of the technologies," *Renewable and Sustainable Energy Reviews*, vol. 14, no. 3, pp. 899–918, Apr. 2010, doi: 10.1016/j.rser.2009.11.003.

[3] A. F. O. Falcão and J. C. C. Henriques, "Oscillating-water-column wave energy converters and air turbines: A review," 2016. doi: 10.1016/j.renene.2015.07.086.

[4] A. W. Lees, *Vibration Problems in Machines*. CRC Press, 2020. doi: 10.1201/9780429351372.

[5] B. Holmes, "Bull Rock," *Sustainable Energy Research Group, HMRC, UCC*, 1984.

[6] "CorPower Ocean - Wave Power. To Power the Planet.," Nov. 2021. [Online]. Available: https://corpowerocean.com

[7] H. Lee and C.-H. Chen, "Parametric Study for an Oscillating Water Column Wave Energy Conversion System Installed on a Breakwater," *Energies (Basel)*, vol. 13, no. 8, p. 1926, Apr. 2020, doi: 10.3390/en13081926.

[8] IEA- International Energy Agency, "Annual Report 2021," 2021.

[9] I. López, B. Pereiras, F. Castro, and G. Iglesias, "Performance of OWC wave energy converters: influence of turbine damping and tidal variability," *Int J Energy Res*, vol. 39, no. 4, pp. 472–483, Mar. 2015, doi: 10.1002/er.3239.

[10] J. M. B. P. Cruz and A.J.N.A. Sarmento, " Energia das Ondas: Introdução aos Aspectos Tecnológicos, Económicos e Ambientais",

Ed. Instituto do Ambiente, Alfragide, 2004. [online]. Available: https://apambiente.pt/sites/default/files/_SNIAMB_A_APA/.

[11] K. Koca *et al.*, "Recent Advances in the Development of Wave Energy Converters," *Conference: The 10th European Wave and Tidal Energy Conference (EWTEC 2013)At: Aalborg, Denmark*, 2013.

[12] L. Del Frate, F. Moretti, G. Galassi, and F. D'Auria, "Limitations in the Use of the Equivalent Diameter," *World Journal of Nuclear Science and Technology*, vol. 06, no. 01, pp. 53–62, 2016, doi: 10.4236/wjnst.2016.61005.

[13] L. Oliveira and A. Lopes, *Mecânica dos Fluidos*, 4a Ed., Lide. 2012.

[14] M. Bošnjaković, M. Katinić, R. Santa, and D. Marić, "Wind Turbine Technology Trends," *Applied Sciences*, vol. 12, no. 17, p. 8653, Aug. 2022, doi: 10.3390/app12178653.

[15] M. A. Krasnosel'skiĭ and A. V. Pokrovskiĭ, *Systems with Hysteresis*. Berlin, Heidelberg: Springer Berlin Heidelberg, 1989. doi: 10.1007/978-3-642-61302-9.

[16] M. Rosati, J. C. C. Henriques, and J. V. Ringwood, "Oscillating-water-column wave energy converters: A critical review of numerical modelling and control," 2022. doi: 10.1016/j.ecmx.2022.100322.

[17] P. Puddu, M. Paderi, and C. Manca, "Aerodynamic Characterization of a Wells Turbine under Bi-directional Airflow," *Energy Procedia*, vol. 45, pp. 278–287, 2014, doi: 10.1016/j.egypro.2014.01.030.

[18] Q. Yao, S. M. Wang, and H. P. Hu, "Development and Prospect of Wave Power Generation Devices," *Ocean Dev. Manag*, vol. 33, pp. 86–92, 2016, [Online]. Available: https://scholar.google.com/scholar_lookup?title=Development+and+ Prospect + of + Wave + Power + Generation + Devices &a uthor = Yao, + Q. & author = Wang,+S.M.& author = Hu,+ H.P. & publication_year= 2016 & journal = Ocean + Dev. + Manag. &volume = 33&pages =86%E2%80%9392

[19] T. Ghisu, F. Cambuli, P. Puddu, I. Virdis, M. Carta, and F. Licheri, "A lumped parameter model to explain the cause of the hysteresis in OWC-Wells turbine systems for wave energy conversion," *Applied Ocean Research*, vol. 94, 2020, doi: 10.1016/j.apor.2019.101994.

[20] T. Ghisu, P. Puddu, and F. Cambuli, "Physical Explanation of the Hysteresis in Wells Turbines: A Critical Reconsideration," *J Fluids Eng*, vol. 138, no. 11, Nov. 2016, doi: 10.1115/1.4033320.

[21] T. Ghisu, P. Puddu, and F. Cambuli, "A detailed analysis of the unsteady flow within a Wells turbine," *Proceedings of the Institution of Mechanical Engineers, Part A: Journal of Power and Energy*, vol. 231, no. 3, pp. 197–214, May 2017, doi: 10.1177/0957650917691640.

[22] T. Setoguchi, M. Takao, and K. Kaneko, "Hysteresis on wells turbine characteristics in reciprocating flow," *International Journal of Rotating Machinery*, vol. 4, no. 1, 1998, doi: 10.1155/S1023621X98000025.

[23] T. R. Kuphaldt., "Lessons in Electric Curcuits, Volume I - DC", 5 ed., ch.6 - Divider Circuits and Kirchhoff's Law," 2006. [Online]. Available: https://www.ibiblio.org/kuphaldt/electricCircuits/DC/index.html

[24] T. R. Kuphaldt, "Lessons in Electric Circuits, Volume I - Direct Current", 5 ed, ch.6 - Divider Circuits and Kirchhoff's Law," 2009. [Online]. Available: https://workforce.libretexts.org/Bookshelves/Electronics_Technology/Book%3A_Electric_Circuits_I_-_Direct_Current_(Kuphaldt)

[25] Z. L. Wang, "New wave power," *Nature 2017 542:7640*, vol. 542, no. 7640, 2017, [Online]. Available : https: //scholar.google.com/scholar_lookup?title = New + wave + power & author = Wang, + Z.L. &publication_year= 2017&journal = Nature & volume = 542 & pages = 159%E2%80%93160&doi=10.1038/542159a

[26] W. M. L. Monteiro and A. J. N. A. Sarmento, ""Cabo Verde Offshore Wave Energy Resources Characterization," *in proc. Of Grand Renewable Energy,Japan*, 2014.

[27] W. M. L. Monteiro, A. Sarmento, C. P. Monteiro, and J. A. L. Monteiro, "Wave energy production by a maritime Natural Cave: performance characterization and the power take-off design," *J Ocean Eng Mar Energy*, vol. 7, no. 3, pp. 327–337, Aug. 2021, doi: 10.1007/s40722-021-00196-w.

[28] W. M. L. Monteiro, A. Sarmento, J. A. L. Monteiro, and C. P. Monteiro, "Wave energy production by a maritime natural cave equipped with Wells turbine," *J Ocean Eng Mar Energy*, vol. 8, no. 3, pp. 457–467, Aug. 2022, doi: 10.1007/s40722-022-00234-1.

[29] W. M. L. Monteiro and A. Sarmento, "Analysing the Possibility of Extracting Energy from Ocean Waves in Cabo-Verde to Produce Clean Electricity - Case-Study: the Leeward Islands," *International Journal of Renewable Energy Development*, vol. 8, no. 1, pp. 103–112, Feb. 2019, doi: 10.14710/ijred.8.1.103-112.

[30] "WaveNet Results from the European Thematic Network on Wave Energy, Final Report, ERK5-CT-1999-20001, European Commission, Energy, Environment and Sustainable Development Programme.," 2003.

[31] Y. Kinoue, T. Setoguchi, T. H. Kim, K. Kaneko, and M. Inoue, "Mechanism of Hysteretic Characteristics of Wells Turbine for Wave Power Conversion," *J Fluids Eng*, vol. 125, no. 2, pp. 302–307, Mar. 2003, doi: 10.1115/1.1538629.

[32] Y. Wang, Y. Yang, and Z. L. Wang, "Triboelectric nanogenerators as flexible power sources," *npj Flexible Electronics*, vol. 1, no. 1, p. 10, Nov. 2017, doi: 10.1038/s41528-017-0007-8.